HHS Public Access

Author manuscript

J Mol Cell Cardiol. Author manuscript; available in PMC 2016 December 29.

Published in final edited form as:

J Mol Cell Cardiol. 2016 March ; 92: 1–9. doi:10.1016/j.yjmcc.2016.01.019.

Increased fibroblast chymase production mediates procollagen autophagic digestion in volume overload

Lianwu Fu[a,c], **Chih-Chang Wei**[a,b], **Pamela C. Powell**[a], **Wayne E. Bradley**[b], **Sarfaraz Ahmad**[d], **Carlos M. Ferrario**[d], **James F. Collawn**[c], and **Louis J. Dell'Italia**[a,b,c,*]

[a]Birmingham Veteran Affairs Medical Center, University of Alabama at Birmingham, Birmingham, AL, United States

[b]Division of Cardiovascular Disease, Department of Medicine, University of Alabama at Birmingham, Birmingham, AL, United States

[c]Department of Cell, Developmental and Integrative Biology, University of Alabama at Birmingham, Birmingham, AL, United States

[d]Division of Surgical Sciences, Wake Forest University School of Medicine, Winston-Salem, NC, United States

Abstract

Background—Previous work has identified mast cells as the major source of chymase largely associated with a profibrotic phenotype. We recently reported increased fibroblast autophagic procollagen degradation in a rat model of pure volume overload (VO). Here we demonstrate a connection between increased fibroblast chymase production and autophagic digestion of procollagen in the pure VO of aortocaval fistula (ACF) in the rat.

Methods and results—Isolated LV fibroblasts taken from 4 and 12 week ACF Sprague–Dawley rats have significant increases in chymase mRNA and chymase activity. Increased intracellular chymase protein is documented by immunocytochemistry in the ACF fibroblasts compared to cells obtained from age-matched sham rats. To implicate VO as a stimulus for chymase production, we show that isolated adult rat LV fibroblasts subjected to 24 h of 20% cyclical stretch induces chymase mRNA and protein production. Exogenous chymase treatment of control isolated adult cardiac fibroblasts demonstrates that chymase is internalized through a dynamin-dependent mechanism. Chymase treatment leads to an increased formation of autophagic vacuoles, LC3-II production, autophagic flux, resulting in increased procollagen degradation. Chymase inhibitor treatment reduces cyclical stretch-induced autophagy in isolated cardiac fibroblasts, demonstrating chymase's role in autophagy induction.

Conclusion—In a pure VO model, chymase produced in adult cardiac fibroblasts leads to autophagic degradation of newly synthesized intracellular procollagen I, suggesting a new role of chymase in extracellular matrix degradation.

*Corresponding author at: Birmingham VA Medical Center, 700 South 19th Street, Birmingham, AL 35233, United States. louis.dellitalia@va.gov (L.J. Dell'Italia).

Disclosures

None.

Keywords

Volume overload; Cardiac fibroblast; Chymase; Autophagy; Intracellular procollagen

1. Introduction

Previous work has identified mast cells as the major source of chymase that has been largely associated with a profibrotic phenotype. In a pure volume overload (VO) induced by aortocaval fistula (ACF) or primary mitral regurgitation (MR), we identified increased chymase and mast cell degranulation at early and late stages in the progression to left ventricular (LV) dilatation, LV wall thinning, cardiomyocyte elongation and thinning, and heart failure [1–4]. We sought to understand the reasons for the net extracellular matrix (ECM) breakdown and lack of replacement of ECM in the pure VO, despite of the upregulation of chymase and other renin-angiotensin system components. In addition to being the major Ang II-forming mechanism in the heart [5–7], chymase activates MMPs [8–11], degrades fibronectin [12] and causes apoptosis of vascular smooth muscle cells and cardiomyocytes through disruption of the focal adhesion complex [13,14]. Until recently, these chymase actions have been assigned to the interstitial compartment within the extracellular matrix. However, we recently demonstrated intracellular chymase in cardiomyocytes during ischemia reperfusion injury in the dog and that the chymase uptake in cardiomyocytes is dynamin-mediated [15].

More recently, we reported increased fibroblast autophagic procollagen degradation in a pure VO rat model [16]. Such a role of autophagy in intracellular procollagen degradation has been demonstrated after TGF-β treatment in primary mesangial cells from mouse kidney [17]. Other studies have demonstrated that chymase is produced in neonatal cardiac fibroblasts under glucose stimulation and is an important Ang II-forming mechanism within the fibroblast [18–20]. In addition, Husain and coworkers [21] showed evidence of chymase production in human cardiac interstitial cells and emphasized the importance of chymase production by endothelial cells and fibroblasts rather than just mast cells alone. Verification of this finding would then elevate the presence and location of chymase from the relatively sparse sites of mast cells in the heart to a more prominent role in juxtaposition to cardiomyocytes throughout the cardiac interstitium.

Here, we demonstrate that chymase is produced within adult cardiac fibroblasts themselves in response to the chronic stress of VO of ACF and in isolated adult cardiac fibroblasts after cyclical stretch. *In vitro* studies in fibroblasts show that chymase addition alone is sufficient to induce autophagy in cardiac fibroblasts and promote intracellular degradation of procollagen without affecting collagen mRNA transcript levels. These studies report a heretofore unrecognized mechanism for chymase production and uptake by fibroblasts and subsequent autophagic degradation of intracellular procollagen. This process exacerbates the ECM homeostatic imbalance by decreasing procollagen production in the face of interstitial collagen degradation and results in net ECM loss and adverse LV remodeling in a pure VO.

2. Experimental methods

2.1. Animal studies

Adult male Sprague–Dawley rats (200–250 g) at 10 weeks old of age were subjected to either sham or ACF surgery as described previously in our laboratory [1–3,22]. Briefly, for induction of ACF, rats were anesthetized with isoflurane (2% O_2 at 2 L/min) 10 min prior to the surgery. A ventral abdominal laparotomy was performed to expose the aorta and caudal vena cava 1.5 cm below the renal arteries. The overlying adventitia was removed by blunt dissection to expose the two vessels, taking care not to disrupt the tissue connecting the vessels. Both vessels were then occluded proximal and distal to the intended puncture site, and an 18-guage needle was inserted into the exposed abdominal aorta and advanced through the medial wall into the vena cava to create the fistula. The needle was withdrawn and the ventral aortic puncture was sealed with cyanoacrylate. Creation of the ACF was visualized by the pulsatile flow of oxygenated blood into the vena cava. The abdominal musculature and skin incisions were closed by standard techniques with absorbable suture and auto clips. The control animals, sham, underwent general anesthesia and an abdominal incision without ACF. Rats were medicated with buprenorphine (0.05 mg/kg; IP) preoperatively and at the end of the day of surgery. Every effort was made to minimize any discomfort to the animals used in these studies. The animals were euthanized following anesthesia with isoflurane and exsanguination by rapid removal of the heart. This method is consistent with the recommendations of the Panel of Euthanasia of the American Veterinary Medical Association. All procedures were approved and performed according to the guidelines of the Institutional Animal Care and Use Committees of the University of Alabama at Birmingham (Animal Resource Program, Protocol 140909,251) and followed the National Institute of Health's "Guide for the Care and Use of Laboratory Animals".

2.2. Cardiac fibroblast isolation

4 or 12 weeks after sham or ACF surgery, adult rat LV fibroblasts were isolated by recirculating perfusion buffer supplemented with 1 mg/ml collagenase type II (Invitrogen, CA) as previously described [1]. Briefly, the heart was perfused with a buffer (120 mM NaCl, 15 mM KCl, 0.5 mM KH_2PO_4, 5 mM $NaHCO_3$, 10 mM HEPES, and 5 mM glucose, at pH 7.0) for 5 min and digested with perfusion buffer containing 1 mg/ml collagenase II for 30 min at 37 °C. The right ventricle and atria were removed before the perfused-heart was minced. The cell suspension was then mixed with stop buffer (perfusion buffer containing 10 mg/ml bovine serum albumin) to prevent further digestion. The cell suspension was added to a mesh cell collector and the flow-through was centrifuged at 80 *g* for 3 min to remove most of the cardiomyocytes. The supernatant containing mainly cardiac fibroblasts was centrifuged at 400 *g* for 8 min then resuspended in DMEM supplemented with antibiotics (penicillin/streptomycin, 1%), L-glutamine ascorbate and 10% FBS. Cells were subjected to differential plating on uncoated cell culture dishes (10 cm diameter) for 90 min. Non-adherent cells (mostly cardiomyocytes, endothelial and smooth muscle cells) were removed. We have demonstrated >95% purity of the prep with very little myofibroblast differentiation [1]. Cultured cells by this protocol routinely showed positive staining for anti-vimentin (Millipore #AB5733; 1:500) and no immunostaining with antibodies to anti-

smooth muscle alpha-actin or fibronectin (1:100 dilutions, Sigma-Aldrich, MO). Adult rat cardiac fibroblasts were used at passages 1 and 2 in the current study.

2.3. Immunocytochemistry (ICC) of cardiac fibroblasts

Immunocytochemistry was performed on adult cardiac fibroblasts isolated from sham or ACF rats, or normal fibroblasts subjected to mechanical stretch (24 h, 20% stretch, 1 Hz) or exposed to recombinant human chymase (2.5 μg/ml for 2 h at 37 °C, Sigma-Aldrich #C8118). The cells were fixed in 4% formaldehyde (Tousimis, Rockville, MD) for 20 min at room temperature (RT) and washed 3 times in PBS, and permeabilized with 0.1% Triton-X-100 (Fisher #BP-151) for 15 min at RT. 10% normal serum (in 1% bovine serum/PBS) for 1 h at RT was used for blocking, followed by overnight incubation at4 °C with a chymase monoclonal (Abcam #ab2377; 1:50) and a vimentin polyclonal antibody (Millipore #AB5733; 1:500). Alexa Fluor 488- and 594-conjugated secondary antibodies (1:700, Life Technologies/Invitrogen, OR) with the appropriate host combinations were incubated for 1 h to stain. Nuclei were stained with DAPI (1.5 μg/ml; Vector Laboratories, CA). Image acquisition and analyzing were performed using a Leica DM6000 epifluorescence microscope and SimplePCI software as described previously [16].

2.4. Cardiac fibroblast chymase activity measurements

Cardiac chymase activity in LV fibroblasts was calculated based on adding 1 nmol/L of highly purified ^{125}I-Ang-(1–12) substrate to the fibroblast plasma membranes and determining the amount of^{125}I-AngIIproduct formation as previously described [29]. Briefly, isolated cardiac fibroblasts were homogenized in assay buffer (containing 25 mM HEPES, 125 mM $NaCl_2$ and 10 μM $ZnCl_2$, pH 7.4) and centrifuged at 44,000 *g* for 60 min to collect the native plasma membranes. The plasma membrane pallet was resuspended in assay buffer. Protein content was measured using the BCA kit. For chymase activity and inhibition studies, the plasma membranes (50–100 μg) were preincubated for 10 min with or without the chymase inhibitor-chymostatin (50 μM) in assay buffer. Besides chymostatin, other inhibitors (Lisinopril for ACE, SCH39373 for neprilysin, MLN-4760 for ACE2, amastatin for aminopeptidases, bestatin for aminopeptidases, benzyl succinate for carboxypeptidases and PCMB for cysteine proteases, each 50 μM) were also added to inhibit the renin-angiotensin enzymes (ACE/ACE2/neprilysin), aminopeptidases and cysteine proteases. After preincubation of plasma membrane with the inhibitor cocktail, radiolabeled ^{125}I-Ang-(1–12) substrate was added into the reaction medium and incubated for an additional 60 min at 37 °C. At the end of the incubation time, the reaction was stopped by adding equal volume of 1% phosphoric acid, mixed well and centrifuged at 28,000 *g* for 20 min to remove the plasma membranes. The clear supernatants were filtered through 0.2 μm PVDF membrane and injected on HPLC C-18 column and ^{125}I-Ang II product generation from ^{125}I-Ang-(1–12) by chymase was measured using an in-line flow-through gamma detector (BioScan Inc., Washington, DC). The enzyme activity was defined as fmoles of Ang II product formed from ^{125}I-Ang-(1–12) substrate per min per mg of protein (fmol Ang II formation/min/mg protein).

2.5. Application of extrinsic mechanical load

Cardiac fibroblasts (50,000 cells/cm^2) were cultured on non-coated Flexcell plates (Flexcell International Corp., Hillsborough, NC, USA) in DMEM medium containing 10% FBS, 2 mM glutamine, 10 U/mL penicillin, and 100 μg/ml streptomycin. The media was changed 24 h before initiation of the experiment and cells were subjected to cyclic strain (1 Hz) on the Flexcell Strain apparatus (model FX-5000; Flexcell International, Hillsborough, NC, USA) at a level of distension sufficient to promote an increment of approximately 20% in surface area at the point of maximal distension on the culture surface. The cyclic stretch was performed for 24 h at 1 Hz without interruptions. In the case of chymase inhibition, the specific chymase inhibitor, TEI-F00806 [15] (100 μM) was added to the medium prior to stretch.

2.6. Chymase and transferrin uptake in cardiac fibroblasts

Rat cardiac fibroblasts were grown for one day in 4-chamber culture slides (BD Falcon, BD Biosciences). The medium was replaced with serum-free medium containing either 0.1% DMSO (vehicle control) or 80 μM dynasore (Selleckchem, MA) and incubated in a 37 °C tissue-culture incubator for 30 min. Recombinant human chymase (2.5 μg/ml, Sigma-Aldrich, MO) or transferrin-Alexa 594 (5 μg/ml, Life Technologies, OR) was added to the medium and incubated for an additional 2 h at 37 °C. The cells were chilled on ice, washed three times with PBS (for the transferrin-Alexa 594 uptake experiments) or with PBS with 0.5 M NaCl (for the chymase uptake experiments) followed by three washes with isotonic PBS, and then fixed with 3% formaldehyde in PBS. The uptake of recombinant human chymase in rat fibroblasts was analyzed by immunocytochemistry. The uptake of transferrin-Alexa 594 was examined directly under fluorescence microscopy using a Leica DM6000 epifluorescence microscope as described above.

2.7. Monitoring autophagy and procollagen degradation by immunoblotting

The increase in autophagy was monitored by immunoblotting with an LC3-specific antibody. Briefly, cardiac fibroblast cells were lysed in RIPA buffer containing protease and phosphatase cocktail inhibitors (Thermo Fisher Scientific, IL). Lysates (10–40 μg) were separated on a 4–20% gradient Bis/Tris gel (Invitrogen, CA) by sodium dodecyl sulfate (SDS)-polyacrylamide gel electrophoresis, transferred to PVDF membranes and probed with primary antibodies overnight (4 °C) and then with appropriate horse-radish-peroxidase-conjugated secondary antibodies (1:2000–1:5000). Bands were visualized by enhanced chemiluminescence (Thermo Fisher Scientific, IL), scanned and analyzed by image J software (NIH, Bethesda, MD). A rabbit polyclonal antibody against LC3 was purchased from Sigma-Aldrich (Cat. # L8918) and used in 1:500 dilutions. Rabbit polyclonal antibody against collagen I was purchased from Abcam (Cat. #ab34710) and used at 1:500 dilution. GAPDH (GeneTax, Cat. #GT239) was used as a loading control for immunoblotting.

2.8. Measurement of autophagic influx

Autophagy flux in cardiac fibroblasts was measured using a plasmid expressing mCherry and GFP-tagged LC3 (pBABE-puro mCherry-EGFP-LC3B; Addgene, 22,418). Cardiac fibroblasts grown on 4-well chamber slides were transfected using Lipofectamine® 3000

Reagent from Invitrogen. 24 h after transfection, the cells were treated with 2.5 μg/ml recombinant human chymase, 5 μM rapamycin, and 100 μM chloroquine for 2 h followed by3%formaldehyde fixation prior to image acquisition as described above. The number of red and green punctate in at least 40 transfected cells in each group were counted using Image Pro Software (MediaCybernetics®). The progression of autophagy is started with the formation of autophagosomes shown as yellow punctate vesicles because they are marked with both red and green fluorescence. When the autophagosomes fuse with the lysosomes to form autolysosomes, the GFP green fluorescent signal is lost because the acidic environment quenches the GFP fluorescence. The augmented appearance of red-only labeled autolysosomes is an indication of the autophagic flux.

2.9. Transmission electron microscopy of cardiac fibroblasts after chymase treatment

Isolated adult cardiac fibroblast cells were treated with 2.5 μg/ml recombinant human chymase for 2 h. Cardiac fibroblasts were then fixed overnight in 2.5% glutaraldehyde in 0.1 M sodium cacodylate buffer (Electron Microscopy Sciences, PA). Transmission electron microscopy (TEM) was performed by EMLABS, Inc., Birmingham, AL. After post-fixation with 1% osmium tetroxide in 0.1 M cacodylate buffer, fibroblasts were dehydrated with a graded series of ethanol and embedded in Epon resin. Semi-thin (0.5 μm) and ultra-thin (90 nm) sections were cut, mounted on copper grids, and post-stained with uranyl acetate and lead citrate. Sections were viewed at 60 kv with a Philips 201 transmission electron microscope (FEI Co., OR) for qualitative changes in the cellular ultrastructure.

2.10. mRNA quantitation by RT-PCR

Total RNA from the cardiac fibroblasts isolated from 4 and 12 week sham and ACF rats, or from isolated control fibroblasts after 24 h of 20% cyclical stretch, or from isolated control fibroblasts treated with recombinant chymase was extracted using the RNeasy Mini Kit (catalog no. 74,106; Qiagen) according to the manufacturer's protocol as previously described [23]. Briefly, mRNA transcripts of chymase and collagen were evaluated by real time RT-PCR using Assay-On-Demand primer mix of Mcpt2 and Col1a1, respectively (Mcpt2, mast cell protease 2, assay ID: Rn00756479_g1; Col1a1, collagen type I, alpha 1, assay ID: Rn01463848_m1). The rat chymase Mcpt2 has 60% identical amino acid sequence comparing to the human chymase CMA1. Ribosomal protein, large, P0 (Rplp0; assay ID: Rn00821065_g1) was used in parallel as internal controls. TaqMan One-Step RT-PCR reactions were performed in 20 μl final volumes containing 5 μl (10× dilution of stock) of RNA sample, AmpErase UNG (2×, 10 μl), MultiScribe reverse transcriptase and RNase inhibitor (40×, 1 μl), primers and probe (20×, 1 μl), and RNase-free water (3 μl). Quantitative real-time PCR was performed using the ABI PRISM 7500 sequence detection system. Chymase and collagen I mRNA levels relative to sham or control were calculated using the ΔΔCt method.

2.11. Statistical analysis

All data were presented as mean ± SEM (standard error of mean). An unpaired Student's t-test was used to compare age-matched shams versus ACF groups and to compare control versus treated groups. One-way ANOVA with Student–Newman–Keuls post hoc test was used in Figs. 6, 7. A p value of less than 0.05 was used for statistical significance.

3. Results

3.1. Chymase is increased in cardiac fibroblasts isolated from the 4 and 12 week ACF rats

Previous studies by our laboratory demonstrated significant LV dilatation in ACF rat hearts at the compensated (4 week) and decompensated stages (12 week) of VO [1–3,16]. Immunohistochemistry demonstrates an increase in intracellular chymase in the cytoplasm and nucleus in 4 and 12 week ACF compared to age-matched shams (Fig. 1A and C). The relative fluorescence intensity of chymase per cell is increased ~8-fold and 10-fold in 4 and 12 week ACF rats, respectively, when compared to age-matched sham controls (Fig. 1B and D). Fibroblast chymase activity, as monitored as chymostatin-inhibitable Ang-II formation using ^{125}I-Ang-(1–12) substrate followed by HPLC analysis (Fig. 2), was increased 20.52 ± 3.81 fmol/min/mg protein and 50.30 ± 11.55 fmol/min/mg protein at 4 and 12 week ACF rats, respectively, compared to age-matched shams. Chymase mRNA was also increased 1.8 ± 0.25-fold and 3.2 ± 0.34-fold in LV fibroblasts isolated from 4 week and 12 week ACF rats, respectively, compared to age-matched shams (Fig. 3). In combination, the results provide evidence for increased fibroblast chymase production and activity in ACF fibroblasts at the compensated and decompensated stages of VO.

3.2. Exogenous chymase is internalized in isolated cardiac fibroblasts

Previous results demonstrate that chymase is taken up into cardiomyocytes by a dynamin-mediated process [15]. Given that chymase is a secreted protein, we also tested for this mode of chymase uptake in isolated adult cardiac fibroblasts. Recombinant human chymase (2.5 μg/mL) was added to isolated adult rat cardiac fibroblasts grown in 4-well chamber slides and incubated for 2 h at 37 °C. The results in Fig. 4A show chymase uptake by the fibroblasts (Fig. 4A, left panel) is blocked by pretreatment with dynasore (80 μM), an inhibitor for dynamin, a GTPase protein that is required for endocytosis (Fig. 4A, right panel). The dynasore pretreatment is also shown to block transferrin uptake by the transferrin receptor, a receptor known to require dynamin for uptake through clathrin-coated pits. The results illustrate that chymase is rapidly taken up by cardiac fibroblasts through a dynamin-mediated endocytic process.

3.3. Exogenous chymase induces autophagy and procollagen degradation in cardiac fibroblasts

We have previously shown that chymase treatment of isolated adult dog cardiomyocytes results in mitochondrial degeneration and autophagic vacuole formation [15]. To test if this occurs in adult rat cardiac fibroblasts, transmission electron microscopy (TEM) and western blot analyses were performed to monitor for autophagy induction and the expression of a marker of autophagosome formation, the type-II microtubule-associated protein 1 light chain 3 (LC3-II). These analyses were performed after a 2-h treatment with recombinant human chymase (2.5 μg/ml). Fig. 5A and B demonstrate that chymase-treated cardiac fibroblasts have a dramatic increase in autophagic vacuoles and the LC3-II production in chymase-treated fibroblasts is increased to 2.59 ± 0.54 fold compared to the control. The increased autophagy was associated with a 42 ± 7% decrease in procollagen I protein as shown by immunoblotting (Fig. 5C) with no apparent change of the collagen I mRNA levels (Fig. 5D). Interestingly, chymase treatment also results in a ~ 60% increase in chymase mRNA as

shown by RT-PCR (Fig. 5E), indicating that exogenous chymase addition to cardiac fibroblasts induces chymase mRNA production in the fibroblasts.

3.4. Chymase induces autophagic flux in cardiac fibroblasts

To further assess the dynamics of autophagy induced by chymase, rat adult cardiac fibroblasts were transfected with a plasmid expressing mCherry-GFP tandem-tagged LC3. The use of this plasmid allows for the differentiation between the formation of autophagosomes (shown in yellow) versus autolysosomes (shown in red), and therefore serves as a measure of autophagic flux in the cells, i.e., the conversion of the former to the latter [24]. Fig. 6 demonstrates that chymase treatment promotes a marked increase of autolysosomes (Fig. 6B, illustrated in red) compared with the control (Fig. 6A). Rapamycin treatment, a known inducer of autophagy, produces results similar to chymase treatment (Fig. 6D). The chymase and rapamycin-induced increase of autolysosome formation is attenuated by chloroquine treatment (CQ, Fig. 6C and E), an inhibitor of the conversion of autophagosomes to autolysosomes. Quantitation of LC3 puncta in at least 40 cells from each group (Fig. 6F) shows that the percentage of red-only autolysosomes is increased from 31.5 ± 6% in control cells to 70.9 ± 2.8% in chymase-treated fibroblasts and to 73.8 ± 2.8% in rapamycin-treated cells. These effects are decreased to 37.4 ± 4% and 29.1 ± 4% with the addition of CQ, respectively. These results demonstrate that chymase treatment, much like rapamycin treatment, induces autophagy that proceeds successfully to the autolysosome stage where protein degradation occurs.

3.5. Mechanical stretch induces chymase expression and autophagy in isolated fibroblasts

To connect pure fibroblast stretch with induction of chymase transcription, we subjected isolated adult rat cardiac fibroblasts to 20% stretch at 1 Hz for 24 h. The results shown in Fig. 7 demonstrate a 3.6-fold increase in chymase protein by immunocytochemistry, particularly in the nuclei (Fig. 7A and B) and nearly a 6-fold increase in chymase mRNA levels after cyclical stretch of adult rat cardiac fibroblasts (Fig. 7C). To establish a connection between chymase and autophagy induction in the cardiac fibroblasts, we treated the fibroblasts with a chymase inhibitor (TEI-F00806, 100 μM) prior to and during the 24 h of cyclical stretch. The results indicated that induction of autophagy by LC3-II production is significantly attenuated by chymase inhibition (Fig. 7D and E). This suggests an autocrine effect mediated by fibroblast chymase production on procollagen degradation.

4. Discussion

The pathophysiologic mechanisms of VO are related to not just an ECM breakdown, but also to a failure to replace ECM, in spite of activation of the profibrotic mechanisms triggered by an increased renin-angiotensin/chymase system [1,25]. Much has been written about the pathophysiologic importance of upregulation of matrix metalloproteinases (MMPs) in ECM breakdown in a pure VO [26–28]. However, we and others have reported a decrease in interstitial collagen and hydroxyproline levels in the ACF rats at 4 and 15 weeks, suggesting a decrease in collagen production [1,3,25]. Here we show that during the course of VO, cardiac fibroblasts produce chymase and that chymase induces a strong autophagic response that leads to increased intracellular degradation of procollagen I. The results of the

current investigation demonstrate a heretofore unrecognized mechanism by which chymase has a negative effect on the production of collagen in VO.

Analysis of compensated and decompensated VO in 4 and 12 week ACF rats demonstrates an increase in chymase mRNA and protein in isolated LV fibroblasts. Furthermore, chymase-mediated Ang II-forming capacity from Ang-(1–12) is increased in these ACF fibroblasts. In addition, cyclical stretch of cardiac fibroblasts results in an increase in chymase mRNA and protein. These results suggest that adult cardiac fibroblasts are an important source of chymase under the hemodynamic stress of a pure VO. In addition to the mast cells that were considered to be the major source of chymase [5], chymase has been reported to be produced in neonatal cardiac fibroblasts under glucose stimulation [18–20] and in cardiac interstitial cells such as endothelial cells and fibroblasts of the human heart failure heart [21]. These findings are consistent with our recent studies demonstrating chymase within atrial myocytes in human atrial appendage tissue [29–31]. The connection of chymase production to hemodynamic stretch is also exemplified by our work demonstrating chymase within left atrial myocytes of humans with enlarged left atria undergoing the MAZE procedure for atrial fibrillation and increasing right and left atrial chymase activity in proportion to the severity of left heart disease in patients [30].

Fibroblasts isolated from ACF rat hearts, after chymase treatment, or after cyclical stretch demonstrate chymase inside the cell, and interestingly, illustrate a prominent location in the nucleus (Figs. 1, 4 and 7). Since chymase is a secreted protein, we speculated that chymase may enter cardiac fibroblasts from extracellular spaces. Indeed, our *in vitro* studies demonstrate exogenous chymase is rapidly internalized to fibroblasts by a dynamin-mediated process as we reported recently in cardiomyocytes [15]. A similar endocytic uptake mechanism has been proposed for neutrophil elastase in human lung tumor cells [32,33], granzyme B in lymphocytes [34] and myeloperoxidase in endothelial cells [35]. In addition to the potential for fibroblast chymase uptake, increased chymase mRNA in fibroblasts in response to ACF or mechanical stretch supports a transcriptionally regulated response in cardiac fibroblasts. However, the mechanism for the nuclear localization of chymase remains to be elucidated. In support of an intra-nuclear renin angiotensin system, renal Ang II receptors have been reported to be predominantly localized to the nucleus after cell surface ligand binding and subsequent internalization, which in turn is linked to nitric oxide production in rat kidney [36]. Future studies will delve into the compartmentalization of chymase within the cell and how chymase-mediated intracellular Ang II formation may be functionally connected to nuclear AT_1 receptors [18].

The current study also demonstrates a new function for chymase in the induction of autophagic digestion of procollagen. First, increased fibroblast chymase in ACF rats is associated with the evidence of increased autophagy as determined by LC3-II elevation and TEM evidence of increased autophagic vacuoles and increased procollagen degradation [16]. Second, to establish that chymase originates from the fibroblasts and is related to autophagy induction, 24-h cyclic stretch of adult rat cardiac fibroblasts *in vitro* recapitulated *in vivo* findings of an increase in chymase and autophagy induction that is blocked by a chymase inhibitor. Third, chymase treatment of control LV fibroblasts also increases LC3-II and autophagic vacuoles by TEM and a decrease in procollagen I levels. These *in vitro*

experiments demonstrate that chymase plays a previously unrecognized role to downgrade the ECM level through the induction of autophagy. Based on previous reports, chymase may induce autophagy through several potential mechanisms. First, chymase may induce autophagy through its Ang-II forming function. It was shown recently by Liu et al. that rat cardiac fibroblasts stimulated with Ang-II have activated autophagy [37]. Second, chymase may induce autophagy indirectly by inducing β-adrenergic and TGF-β signaling pathways. Both have been shown to stimulate autophagy in rat cardiac fibroblasts [38] and mouse kidney mesangial cells [17], respectively. Another explanation is that chymase breakdown of fibronectin and the focal adhesion complex may generate an outside-in signal to induce autophagy. This chymase-mediated reaction has been shown to be initiated from the cell surface and has been implicated in apoptosis in isolated smooth muscle cells [14] and in our previous studies in the pure VO in the rat [39] and dog [40].

The fibroblast is the most plentiful cell type in the heart and is the source of ECM proteins, MMPs and tissue inhibitors of MMPs (TIMPs) [41]. Chymase-mediated Ang II formation, MMP activation, and fibronectin degradation have been thought to occur in the cardiac interstitial space. The ability to produce chymase and its potential role in autophagic procollagen degradation opens a new paradigm of the fibroblast in ECM homeostasis. The significance of these findings underscores the ability of fibroblasts to produce chymase and to induce procollagen degradation and supports the wide range of dynamic functional and phenotypic alterations of fibroblasts including cytokine production and transformation in response to various cardiac stresses [42–44]. Given the extensive distribution of fibroblasts compared to mast cells in cardiac tissue, these results now emphasize the importance of fibroblast chymase in the LV remodeling process in VO. It is therefore anticipated that inhibition of chymase will have therapeutic benefits for various heart disease of LV dysfunction. Our recent report demonstrates significant improvement in LV remodeling and function achieved by addition of chymase inhibition to ACE inhibition over ACE inhibition alone in experimental myocardial infarction in the hamster [45]. Furthermore, renin inhibitors, ACE inhibitors, and Ang II receptor blockers have fallen short of expectations in the long-term treatment of cardiovascular disease [46]. Currently, a new type of chymase inhibitor, BAY1142524, is in phase-II clinic trial (NCT02452515 — clinicaltrials.gov) to treat patients with LV dysfunction after myocardial infarction. However, our data suggests chymase has intracellular functions to regulate the ECM production. Understanding all of the intracellular functions of chymase in both cardiac fibroblasts and myocytes is clearly an important next step that requires careful examination since these intracellular chymase-mediated functions might be divergent from ACE inhibitors or type 1 Ang II receptor blockers which act at the cell surface.

Acknowledgments

Funding

This work was supported by grants from Department of Veteran Affairs for Merit Review (Grant 1BX001050-01 to C.C.W. and Grant 1CX000993-01 to L.J.D.) and NIH (Grant P01 HL051952 to CMF and L.J.D.).

References

1. Wei CC, Chen Y, Powell LC, Zheng J, Shi K, Bradley WE, et al. Cardiac kallikreinkinin system is upregulated in chronic volume overload and mediates an inflammatory induced collagen loss. PLoS ONE. 2012; 7:e40110. [PubMed: 22768235]
2. Ryan TD, Rothstein EC, Aban I, Tallaj JA, Husain A, Lucchesi PA, et al. Left ventricular eccentric remodeling and matrix loss are mediated by bradykinin and precede cardiomyocyte elongation in rats with volume overload. J Am Coll Cardiol. 2007; 49:811–821. [PubMed: 17306712]
3. Chen YW, Pat B, Gladden JD, Zheng J, Powell P, Wei CC, et al. Dynamic molecular and histopathological changes in the extracellular matrix and inflammation in the transition to heart failure in isolated volume overload. Am J Physiol Heart Circ Physiol. 2011; 300:H2251–H2260. [PubMed: 21421827]
4. Dell'Italia LJ, Meng QC, Balcells E, Wei CC, Palmer R, Hageman GR, et al. Compartmentalization of angiotensin II generation in the dog heart. Evidence for independent mechanisms in intravascular and interstitial spaces. J Clin Invest. 1997; 100:253–258. [PubMed: 9218500]
5. Dell'Italia LJ, Husain A. Dissecting the role of chymase in angiotensin II formation and heart and blood vessel diseases. Curr Opin Cardiol. 2002; 17:374–379. [PubMed: 12151872]
6. Urata H, Healy B, Stewart RW, Bumpus FM, Husain A. Angiotensin II-forming pathways in normal and failing human hearts. Circ Res. 1990; 66:883–890. [PubMed: 2156635]
7. Urata H, Kinoshita A, Misono KS, Bumpus FM, Husain A. Identification of a highly specific chymase as the major angiotensin II-forming enzyme in the human heart. J Biol Chem. 1990; 265:22348–22357. [PubMed: 2266130]
8. Urata H. Chymase and matrix metalloproteinase. Hypertens Res. 2007; 30:3–4. [PubMed: 17460365]
9. Fang KC, Raymond WW, Blount JL, Caughey GH. Dog mast cell alpha-chymase activates progelatinase B by cleaving the Phe88-Gln89 and Phe91-Glu92 bonds of the catalytic domain. J Biol Chem. 1997; 272:25628–25635. [PubMed: 9325284]
10. Fang KC, Raymond WW, Lazarus SC, Caughey GH. Dog mastocytoma cells secrete a 92-kD gelatinase activated extracellularly by mast cell chymase. J Clin Invest. 1996; 97:1589–1596. [PubMed: 8601622]
11. Saarinen J, Kalkkinen N, Welgus HG, Kovanen PT. Activation of human interstitial procollagenase through direct cleavage of the Leu83-Thr84 bond by mast cell chymase. J Biol Chem. 1994; 269:18134–18140. [PubMed: 8027075]
12. Vartio T, Seppa H, Vaheri A. Susceptibility of soluble and matrix fibronectins to degradation by tissue proteinases, mast cell chymase and cathepsin G. J Biol Chem. 1981; 256:471–477. [PubMed: 6450204]
13. Hara M, Matsumori A, Ono K, Kido H, Hwang MW, Miyamoto T, et al. Mast cells cause apoptosis of cardiomyocytes and proliferation of other intramyocardial cells in vitro. Circulation. 1999; 100:1443–1449. [PubMed: 10500047]
14. Leskinen MJ, Lindstedt KA, Wang Y, Kovanen PT. Mast cell chymase induces smooth muscle cell apoptosis by a mechanism involving fibronectin degradation and disruption of focal adhesions. Arterioscler Thromb Vasc Biol. 2003; 23:238–243. [PubMed: 12588765]
15. Zheng J, Wei CC, Hase N, Shi K, Killingsworth CR, Litovsky SH, et al. Chymase mediates injury and mitochondrial damage in cardiomyocytes during acute ischemia/reperfusion in the dog. PLoS ONE. 2014; 9:e94732. [PubMed: 24733352]
16. Fu L, Wei CC, Powell PC, Bradley WE, Collawn JF, Dell'Italia LJ. Volume overload induces autophagic degradation of procollagen in cardiac fibroblasts. J Mol Cell Cardiol. 2015; 89(Pt B): 241–50. [PubMed: 26596413]
17. Kim SI, Na HJ, Ding Y, Wang Z, Lee SJ, Choi ME. Autophagy promotes intracellular degradation of type I Collagen induced by transforming growth factor (TGF)-beta1. J Biol Chem. 2012; 287:11677–11688. [PubMed: 22351764]
18. Singh VP, Baker KM, Kumar R. Activation of the intracellular renin-angiotensin system in cardiac fibroblasts by high glucose: role in extracellular matrix production. Am J Physiol Heart Circ Physiol. 2008; 294:H1675–H1684. [PubMed: 18296558]

19. Singh VP, Le B, Bhat VB, Baker KM, Kumar R. High-glucose-induced regulation of intracellular ANG II synthesis and nuclear redistribution in cardiac myocytes. Am J Physiol Heart Circ Physiol. 2007; 293:H939–H948. [PubMed: 17483239]
20. Re RN, Cook JL. Noncanonical intracrine action. J Am Soc Hypertens. 2011; 5:435–448. [PubMed: 21890449]
21. Urata H, Boehm KD, Philip A, Kinoshita A, Gabrovsek J, Bumpus FM, et al. Cellular localization and regional distribution of an angiotensin II-forming chymase in the heart. J Clin Invest. 1993; 91:1269–1281. [PubMed: 7682566]
22. Wei CC, Lucchesi PA, Tallaj J, Bradley WE, Powell PC, Dell'Italia LJ. Cardiac interstitial bradykinin and mast cells modulate pattern of LV remodeling in volume overload in rats. Am J Physiol Heart Circ Physiol. 2003; 285:H784–H792. [PubMed: 12663259]
23. Rab A, Bartoszewski R, Jurkuvenaite A, Wakefield J, Collawn JF, Bebok Z. Endoplasmic reticulum stress and the unfolded protein response regulate genomic cystic fibrosis transmembrane conductance regulator expression. Am J Physiol Cell Physiol. 2007; 292:C756–C766. [PubMed: 16987996]
24. Volpicelli-Daley LA, Luk KC, Lee VM. Addition of exogenous alpha-synuclein preformed fibrils to primary neuronal cultures to seed recruitment of endogenous alpha-synuclein to Lewy body and Lewy neurite-like aggregates. Nat Protoc. 2014; 9:2135–2146. [PubMed: 25122523]
25. Ruzicka M, Keeley FW, Leenen FH. The renin-angiotensin system and volume overload-induced changes in cardiac collagen and elastin. Circulation. 1994; 90:1989–1996. [PubMed: 7923689]
26. Hutchinson KR, Guggilam A, Cismowski MJ, Galantowicz ML, West TA, Stewart JA Jr, et al. Temporal pattern of left ventricular structural and functional re-modeling following reversal of volume overload heart failure. J Appl Physiol (1985). 2011; 111:1778–1788. [PubMed: 21885799]
27. Brower GL, Chancey AL, Thanigaraj S, Matsubara BB, Janicki JS. Cause and effect relationship between myocardial mast cell number and matrix metalloproteinase activity. Am J Physiol Heart Circ Physiol. 2002; 283:H518–H525. [PubMed: 12124196]
28. Stewart JA Jr, Wei CC, Brower GL, Rynders PE, Hankes GH, Dillon AR, et al. Cardiac mast cell- and chymase-mediated matrix metalloproteinase activity and left ventricular remodeling in mitral regurgitation in the dog. J Mol Cell Cardiol. 2003; 35:311–319. [PubMed: 12676546]
29. Ahmad S, Simmons T, Varagic J, Moniwa N, Chappell MC, Ferrario CM. Chymase-dependent generation of angiotensin II from angiotensin-(1-12) in human atrial tissue. PLoS ONE. 2011; 6:e28501. [PubMed: 22180785]
30. Nagata S, Varagic J, Kon ND, Wang H, Groban L, Simington SW, et al. Differential expression of the angiotensin-(1-12)/chymase axis in human atrial tissue. Ther Adv Cardiovasc Dis. 2015; 9:168–180. [PubMed: 26082339]
31. Ferrario CM, Ahmad S, Nagata S, Simington SW, Varagic J, Kon N, et al. An evolving story of angiotensin-II-forming pathways in rodents and humans. Clin Sci (Lond). 2014; 126:461–469. [PubMed: 24329563]
32. Houghton AM, Rzymkiewicz DM, Ji H, Gregory AD, Egea EE, Metz HE, et al. Neutrophil elastase-mediated degradation of IRS-1 accelerates lung tumor growth. Nat Med. 2010; 16:219–223. [PubMed: 20081861]
33. Gregory AD, Hale P, Perlmutter DH, Houghton AM. Clathrin pit-mediated endocytosis of neutrophil elastase and cathepsin G by cancer cells. J Biol Chem. 2012; 287:35341–35350. [PubMed: 22915586]
34. Veugelers K, Motyka B, Goping IS, Shostak I, Sawchuk T, Bleackley RC. Granule-mediated killing by granzyme B and perforin requires a mannose 6-phosphate receptor and is augmented by cell surface heparan sulfate. Mol Biol Cell. 2006; 17:623–633. [PubMed: 16280358]
35. Baldus S, Eiserich JP, Mani A, Castro L, Figueroa M, Chumley P, et al. Endothelial transcytosis of myeloperoxidase confers specificity to vascular ECM proteins as targets of tyrosine nitration. J Clin Invest. 2001; 108:1759–1770. [PubMed: 11748259]
36. Gwathmey TM, Shaltout HA, Pendergrass KD, Pirro NT, Figueroa JP, Rose JC, et al. Nuclear angiotensin II type 2 (AT2) receptors are functionally linked to nitric oxide production. Am J Physiol Renal Physiol. 2009; 296:F1484–F1493. [PubMed: 19244399]

37. Liu S, Chen S, Li M, Zhang B, Shen P, Liu P, et al. Autophagy activation attenuates angiotensin II-induced cardiac fibrosis. Arch Biochem Biophys. 2015; 590:37–47. [PubMed: 26562437]
38. Aranguiz-Urroz P, Canales J, Copaja M, Troncoso R, Vicencio JM, Carrillo C, et al. Beta(2)-adrenergic receptor regulates cardiac fibroblast autophagy and collagen degradation. Biochim Biophys Acta. 2011; 1812:23–31. [PubMed: 20637865]
39. Seqqat R, Guo X, Rafiq K, Kolpakov MA, Guo J, Koch WJ, et al. Beta1-adrenergic receptors promote focal adhesion signaling downregulation and myocyte apoptosis in acute volume overload. J Mol Cell Cardiol. 2012; 53:240–249. [PubMed: 22609523]
40. Pat B, Chen Y, Killingsworth C, Gladden JD, Shi K, Zheng J, et al. Chymase inhibition prevents fibronectin and myofibrillar loss and improves cardiomyocyte function and LV torsion angle in dogs with isolated mitral regurgitation. Circulation. 2010; 122:1488–1495. [PubMed: 20876440]
41. Banerjee I, Fuseler JW, Price RL, Borg TK, Baudino TA. Determination of cell types and numbers during cardiac development in the neonatal and adult rat and mouse. Am J Physiol Heart Circ Physiol. 2007; 293:H1883–H1891. [PubMed: 17604329]
42. Chen W, Frangogiannis NG. Fibroblasts in post-infarction inflammation and cardiac repair. Biochim Biophys Acta. 2013; (1833):945–953. [PubMed: 22982064]
43. Nam YJ, Song K, Luo X, Daniel E, Lambeth K, West K, et al. Reprogramming of human fibroblasts toward a cardiac fate. Proc Natl Acad Sci U S A. 2013; 110:5588–5593. [PubMed: 23487791]
44. Song K, Nam YJ, Luo X, Qi X, Tan W, Huang GN, et al. Heart repair by reprogramming non-myocytes with cardiac transcription factors. Nature. 2012; 485:599–604. [PubMed: 22660318]
45. Wei CC, Hase N, Inoue Y, Bradley EW, Yahiro E, Li M, et al. Mast cell chymase limits the cardiac efficacy of Ang I-converting enzyme inhibitor therapy in rodents. J Clin Invest. 2010; 120:1229–1239. [PubMed: 20335663]
46. Turnbull F, Neal B, Ninomiya T, Algert C, Arima H, Barzi F, et al. Effects of different regimens to lower blood pressure on major cardiovascular events in older and younger adults: meta-analysis of randomised trials. BMJ. 2008; 336:1121–1123. [PubMed: 18480116]

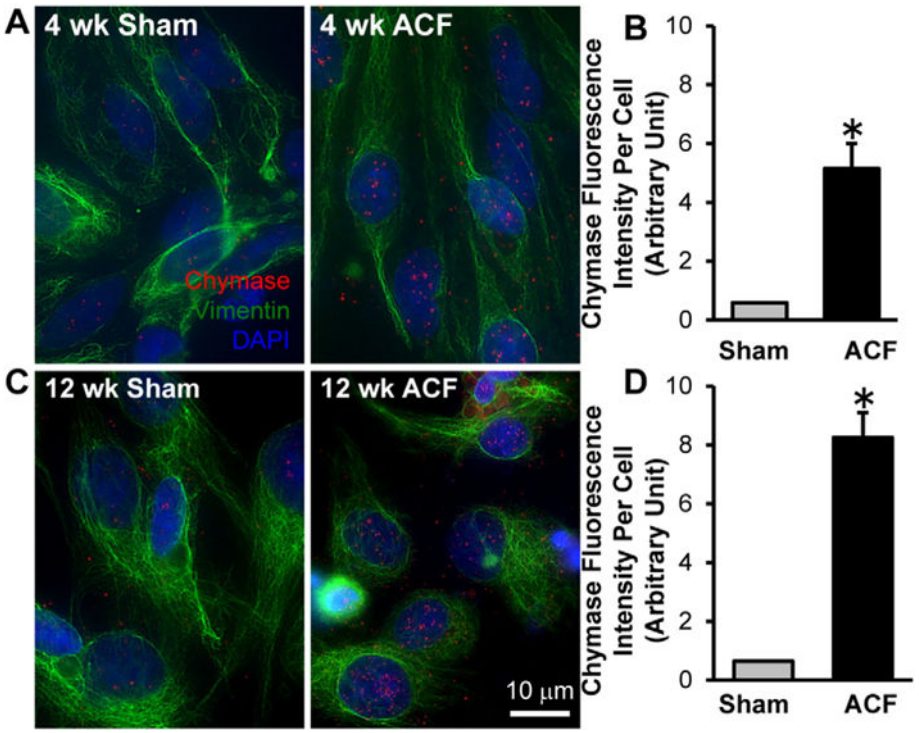

Fig. 1.

Chymase protein is increased in cardiac fibroblasts isolated from 4 and 12 week ACF rats compared to age-matched shams as shown by Immunocytochemistry. Cardiac fibroblasts were isolated from 4 week (A) and 12 week (C) sham and ACF rats followed by indirect fluorescence microcopy using chymase (red) and vimentin (green) antibodies. DAPI: blue. Quantitation of chymase fluorescence intensity in at least 40 cells demonstrates a marked increase in chymase protein in fibroblasts isolated from 4 week (B) and 12 week (D) ACF rats compared to the age-matched shams.

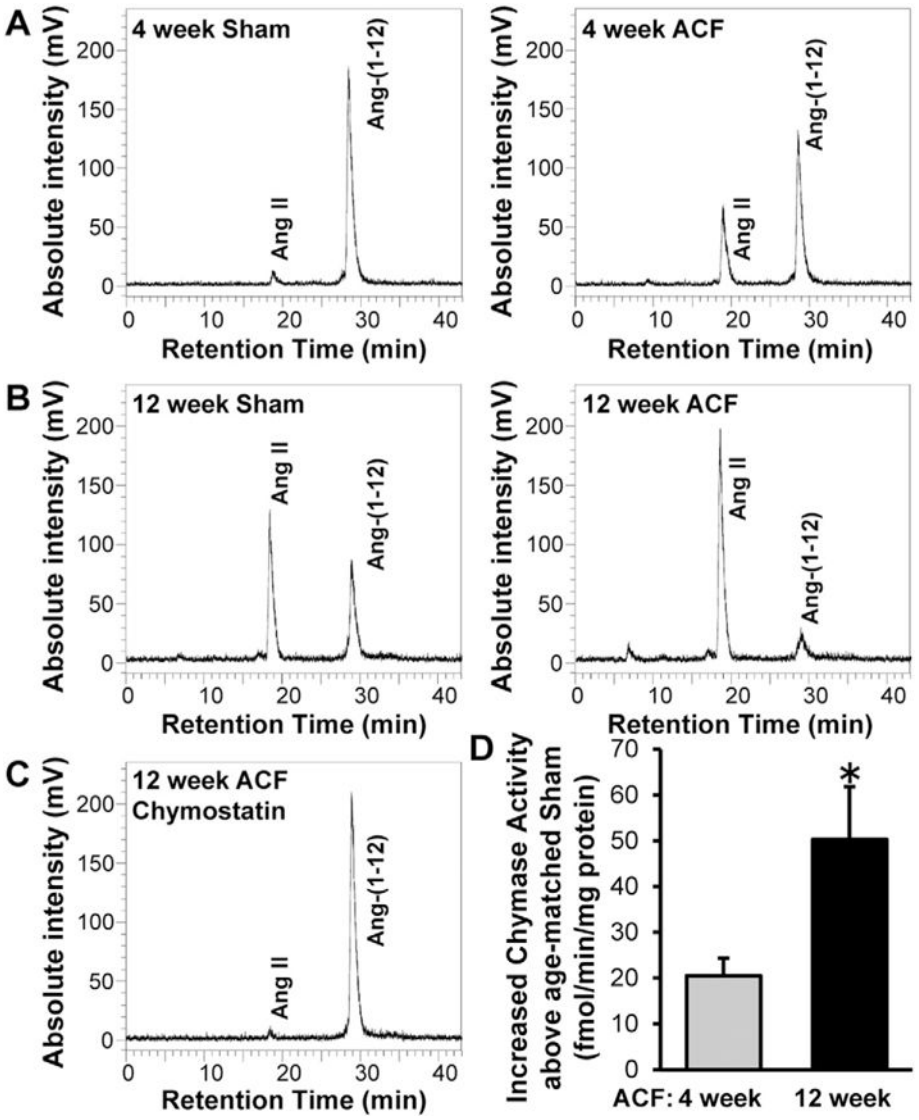

Fig. 2.

Chymase activity is increased in cardiac fibroblasts isolated from 4 and 12 week ACF rats compared to age-matched shams. Cardiac fibroblasts were isolated from 4 week (A) and 12 week (B) sham and ACF rats were analyzed for chymase activity as described in the Experimental methods section. (A, B) Representative HPLC chromatograms showing chymase activity based on ^{125}I-Ang-II formation from the hydrolysis of ^{125}I-Ang-(1–12). The increased chymase activity is blocked when chymostatin is presented in the reaction mixture (C). (D) Bar graph demonstrates that chymase activity is increased in cardiac fibroblast cells isolated from 4 and 12 week ACF rats compared to age-matched shams. n = 4 each. There is also a significant increase in chymase activity in 12 week ACF fibroblasts vs. 4 week ACF fibroblasts. *$P < 0.05$.

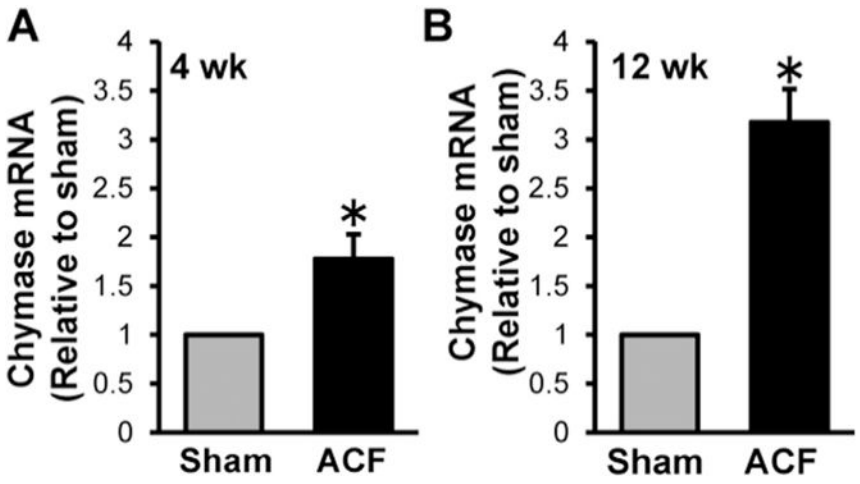

Fig. 3.

Chymase mRNA is increased in cardiac fibroblasts isolated from 4 and 12 week ACF rats compared to age-matched shams. Cardiac fibroblasts were isolated from 4 week (A) and 12 week (B) sham and ACF rats were analyzed for chymase mRNA by real-time PCR as described in the Experimental methods section. There is a marked increase of chymase mRNA in cardiac fibroblasts isolated from ACF rats. n = 6 each. $*P < 0.05$.

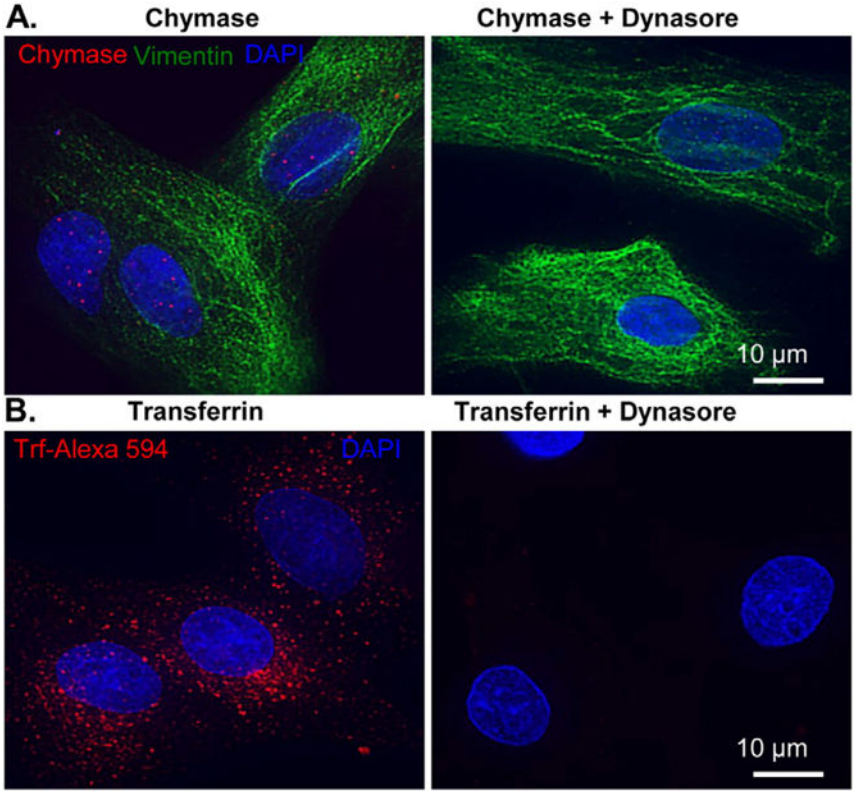

Fig. 4.

Exogenous chymase is internalized to adult cardiac fibroblasts through dynamin-mediated endocytosis. (A), Adult rat cardiac fibroblast cells were incubated with recombinant human chymase (2.5 μg/ml) for 2 h followed by ICC analysis with anti-chymase (red) and anti-vimentin (green) antibodies. There is marked chymase entry into the cytoplasm and nuclei of the fibroblasts (left panel) that is prevented by pretreatment with dynasore, a dynamin inhibitor (80 μM, right panel). (B), Control experiments reveal that dynasore treatment prevents transferrin uptake by fibroblasts. Rat cardiac fibroblasts were incubated with 5 μg/ml transferrin-Alexa 594 (red) for 2 h followed by fluorescence microscopy. There is marked entry of transferrin into the fibroblast cytoplasm (left panel) that is prevented by pretreatment with dynasore (right panel). n = 3. DAPI: blue.

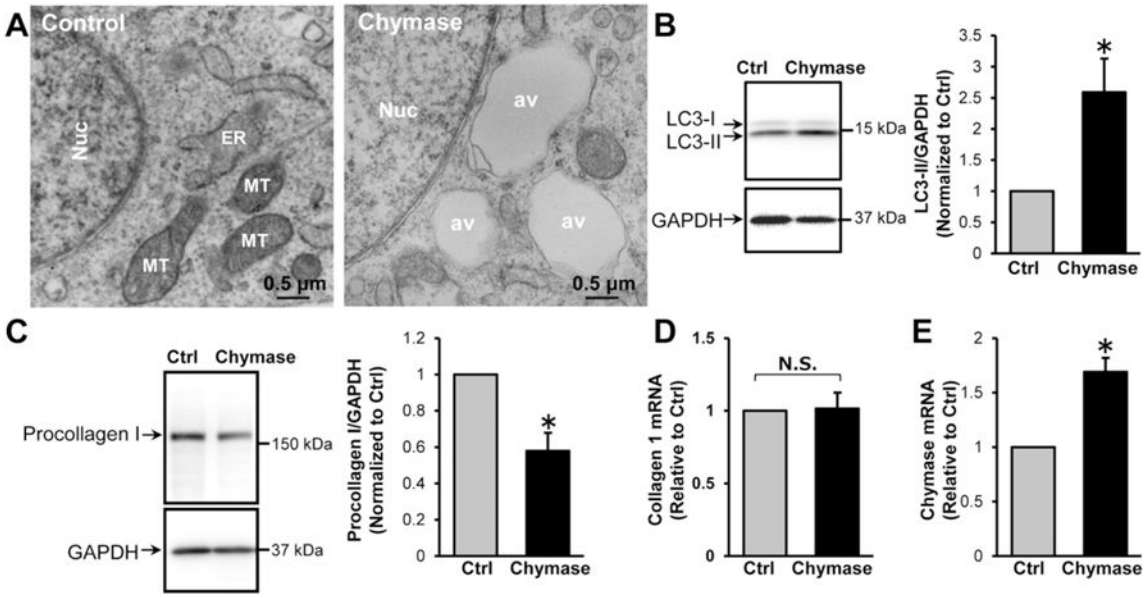

Fig. 5.

Chymase treatment induces autophagy and procollagen degradation in cardiac fibroblasts. (A), Adult rat cardiac fibroblasts were treated with chymase (2.5 μg/ml) for 2 h and then processed for TEM analyses. There is a marked increase of autophagic vacuoles. av: autophagic vacuoles; Nuc: nucleus; ER: rough endoplasmic reticulum; MT: mitochondria. (B), The expression of an autophagic marker, LC3-II, was analyzed by immunoblotting. Chymase treatment increases LC3-II expression, n = 4. (C), Chymase treatment results in a 50% reduction of procollagen I protein as measured by immunoblotting with no change in collagen I mRNA as shown by RT-PCR (D), n = 4, N.S.: not significant. (E) Chymase treatment increases chymase mRNA as shown by RT-PCR. n = 4, $*P < 0.05$ vs. control.

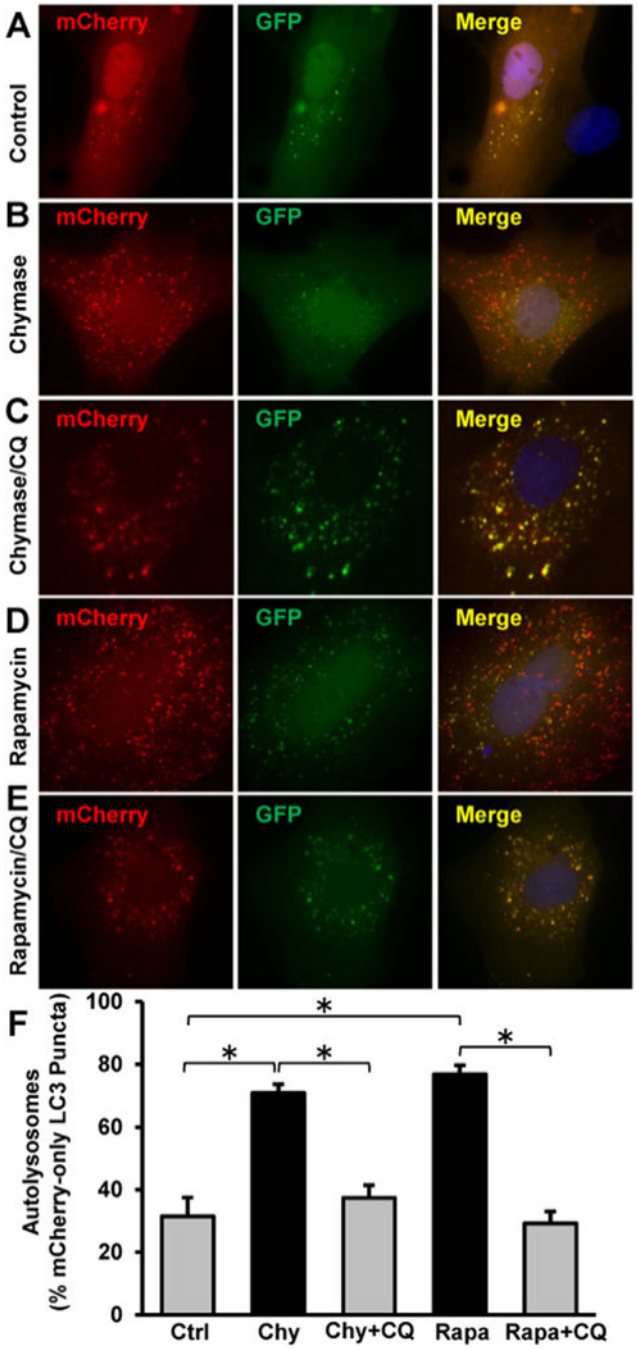

Fig. 6.

Chymase induces autophagic flux in adult cardiac fibroblasts. Adult cardiac fibroblast cells grown on 4-well chamber slides were transfected with the plasmid expressing mCherry-GFP-LC3 as described in the Experimental methods. 24 h after transfection, the cells were treated for 2 h with (A) mock control, (B) 2.5 μg/ml recombinant chymase (Chy), (C) Chymase and 100 μM chloroquine (CQ), (D) 5 μM Rapamycin (Rapa), or (E) 5 μM Rapamycin and CQ. The formation of autophagosomes and autolysosomes during autophagy process was analyzed by fluorescence microscopy. (F), Quantitation of red-only

puncta in at least 40 transfected cells from each group demonstrates an increased autophagic flux in cardiac fibroblasts treated with chymase or rapamycin. *$P < 0.05$.

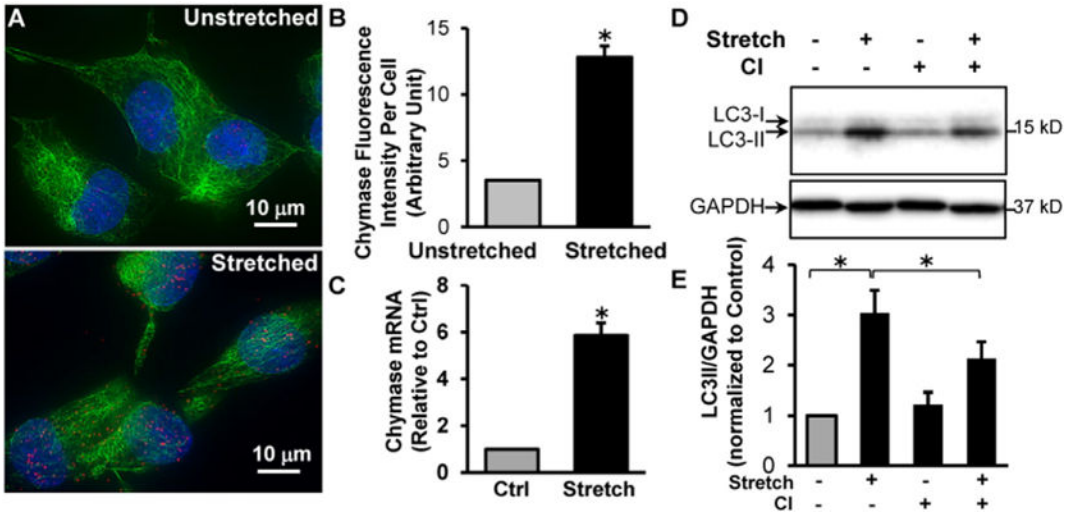

Fig. 7.

Mechanical stretch of adult rat cardiac fibroblasts induces chymase production and autophagy that is inhibited by a chymase inhibitor. Adult rat LV fibroblasts cultured in Flexcell plates were subjected to 20% cyclic stretch (1 Hz) for 24 h. (A), Representative images of ICC shows an increased chymase protein in stretched fibroblasts. Chymase: red; Vimentin: green; Blue: DAPI. (B), Quantitation of fluorescence intensity of at least 40 cells demonstrates a 3.6-fold increase of chymase protein upon stretch. (C), Quantitative RT-PCR shows a ~ 6 fold increase of chymase mRNA after stretch. (D), Adult cardiac fibroblasts were pretreated with 100 μM chymase inhibitor (TEI-F00806) and subjected to cyclic stretch for 24 h. Western blot demonstrates that stretch-induced LC3-II production is attenuated by chymase inhibitor. (E), Bar graph shows the results of 4 experiments. $*P < 0.05$.